4. DATA COLLECTION AND PROCESSING

This section describes the data collection and processing of the data taken for the penetration measurements.

4.1 Data Collection

The data collection for all sites consisted of recording received signal level at each frequency at a rate of one sample per second for the period of time it took the cart to traverse the desired path length for each particular room or hallway. The cart was moving at a speed of approximately 0.5 m/s. All receivers and transmitters at the three frequencies were operating simultaneously. The antennas were oriented in a line and the cart was positioned so that all antennas had a clear field of view of the van in a manner such that none of the antennas were blocking each other. For the Radio Building Stockroom, the signal level was recorded as the cart was moved along two paths within the room. One was parallel to the line-of-sight path between the van and the cart and the other was perpendicular to this line-of-sight path. For the private residence (the wood-frame house), the cart moved along only one path perpendicular to the line-of-site between the van and the cart for the measurement. Measurements of all cart/van distances at each sample site were obtained so that the distance to the van could be determined and the free-space signal level could be calculated at that particular distance. This free-space signal level was then subtracted from the measured data to determine the building penetration loss.

The data were stored in separate files for each of the paths in each room. For example, there were a number of files recorded for each of two orthogonal paths within an office. The data were recorded in separate files for each of three frequencies. A start and stop time was also part of the data. A description of what the data are and how the data were taken is also correlated with the file name. The files can be treated separately or combined in any number of meaningful combinations. This could include: hallway data only, office data only, data taken moving through all the stations along the length of the hallway, or the total of all data taken in a particular building type. The files are listed separately and can be combined to look at effects covering certain situations. During analysis, the data can be separated by functional experiment or combined together.

4.2 Data Processing

The data taken during the collection path runs for any of the building structures were processed to remove the free-space loss from the measurements. This was done by putting coordinates on the layout of each structure to locate all positions on the path in an x-y coordinate system with reference to the van location. The radial distance from the van could then be determined for each particular data point from the geometry. The free-space signal level for each particular data point is then corrected for free-space loss by using the measured free-space calibration signal level at a reference distance and adding the value necessary to correct to the radial distance between the van and the particular data point. This value in decibels is 20*log(R/Ro), where Ro is the reference distance at which the free-space calibration was taken, and R is the actual radial distance of the particular data point under consideration. The measured signal level at the particular data point is then subtracted from the free-space signal level to obtain the attenuation through the structure.

Figures 10, 11, and 12 are examples of this process for each of the three frequencies: 900 MHz, 11.4 GHz, and 28.8 GHz. Each figure demonstrates what has been done to the data files. The raw data, free-space correction factor, and final penetration attenuation are shown in each figure. The position on the horizontal axis is the distance in meters traversed along the path.

The penetration attenuation for all paths in the three building structures at the three frequencies was then plotted for analytical purposes. The data were also examined statistically. This is discussed in the next section.

5. DISCUSSION OF RESULTS

The attenuation versus distance traversed for all three frequencies was also plotted for each of the path runs made in all three building structures. Figures 13, 14, and 15 show selected runs for this penetration loss comparison. Figure 13 is a typical run for one of the paths taken in the Radio Building. Figure 14 is a typical run for one of the paths taken in the storeroom building with metal siding. Figure 15 is a typical run for the private residence (single-level wood-frame house with brick veneer). The complete set of attenuation plots for all paths is contained in the Appendix A. The paths in Figures 10 through 15, as well as those figures in Appendix A, are keyed by an alphanumeric code corresponding to those given in the floor-plan Figures 7, 8, and 9 to identify the runs. These plots provide a direct comparison of the penetration attenuation for the three frequencies in each of the three building structures.

Statistical analyses of the separate paths, as well as combinations of these paths, were performed to better characterize the data. The mean and standard deviation of the mean are summarized in Table 1 for the Radio Building, Table 2 for the private residence, and Table 3 for the storeroom. Table 4 contains the results for selected combinations of paths for each of the three building structures. The codes for the paths listed in the first column of

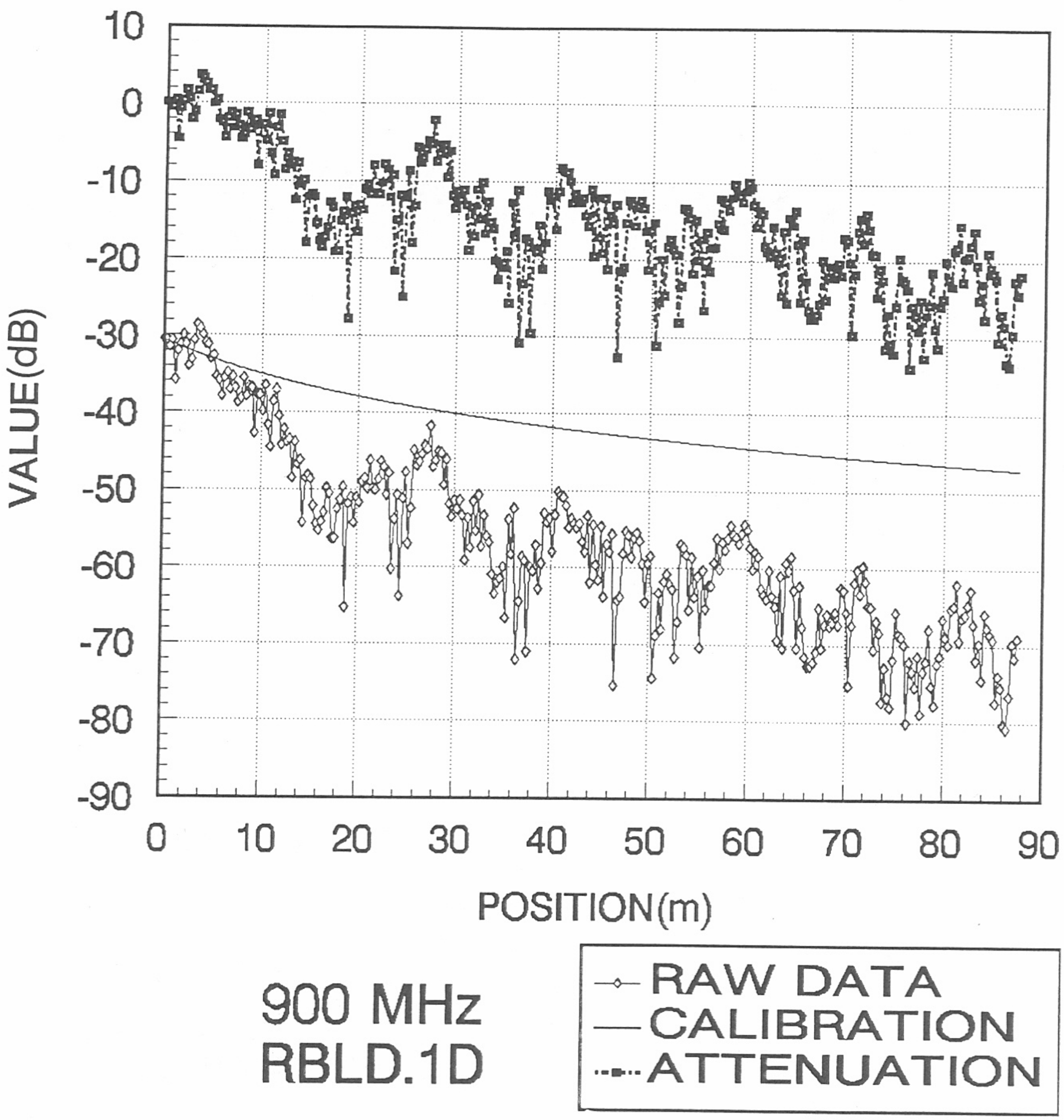

Figure 10. Raw data, free-space correction factor, and penetration attenuation versus distance for a typical 900-MHz measurement in the Radio Building.

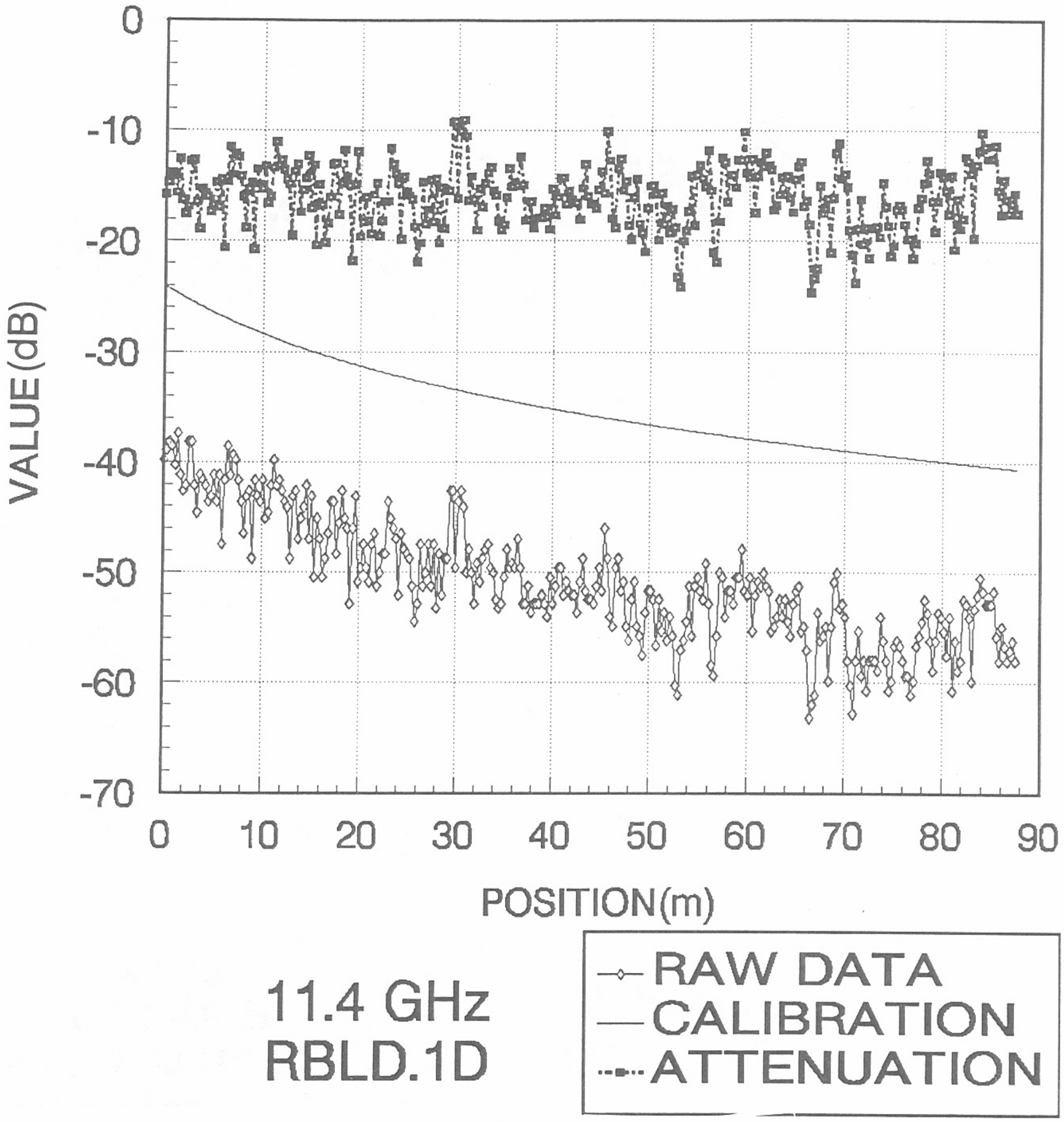

Figure 11. Raw data, free-space correction factor, and penetration attenuation versus distance for a typical 11.4-GHz measurement in the Radio Building.

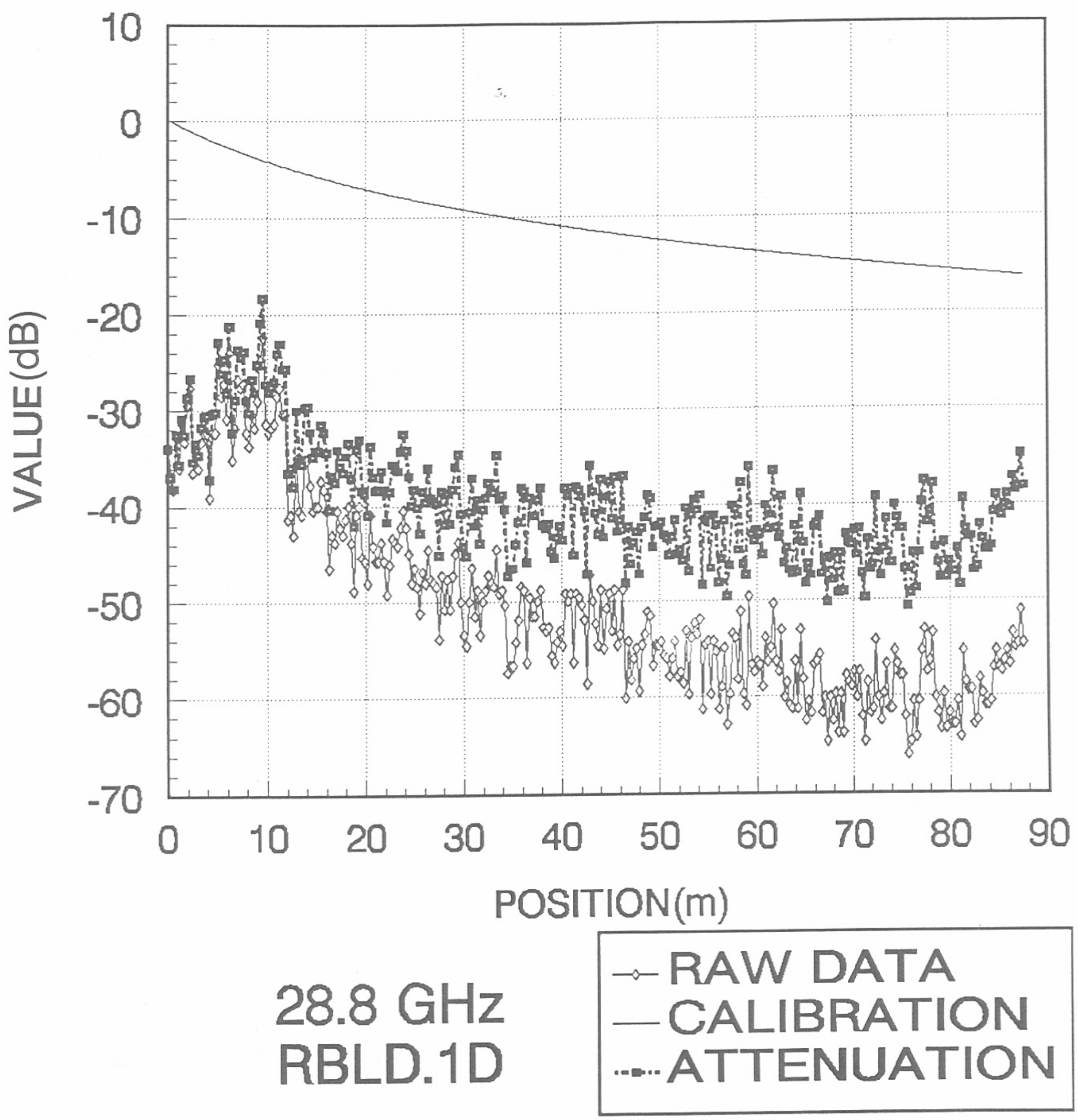

Figure 12. Raw data, free-space corection factor, and penetration attenuation versus distance for a typical 28.4 GHz measurement in the Radio Building.

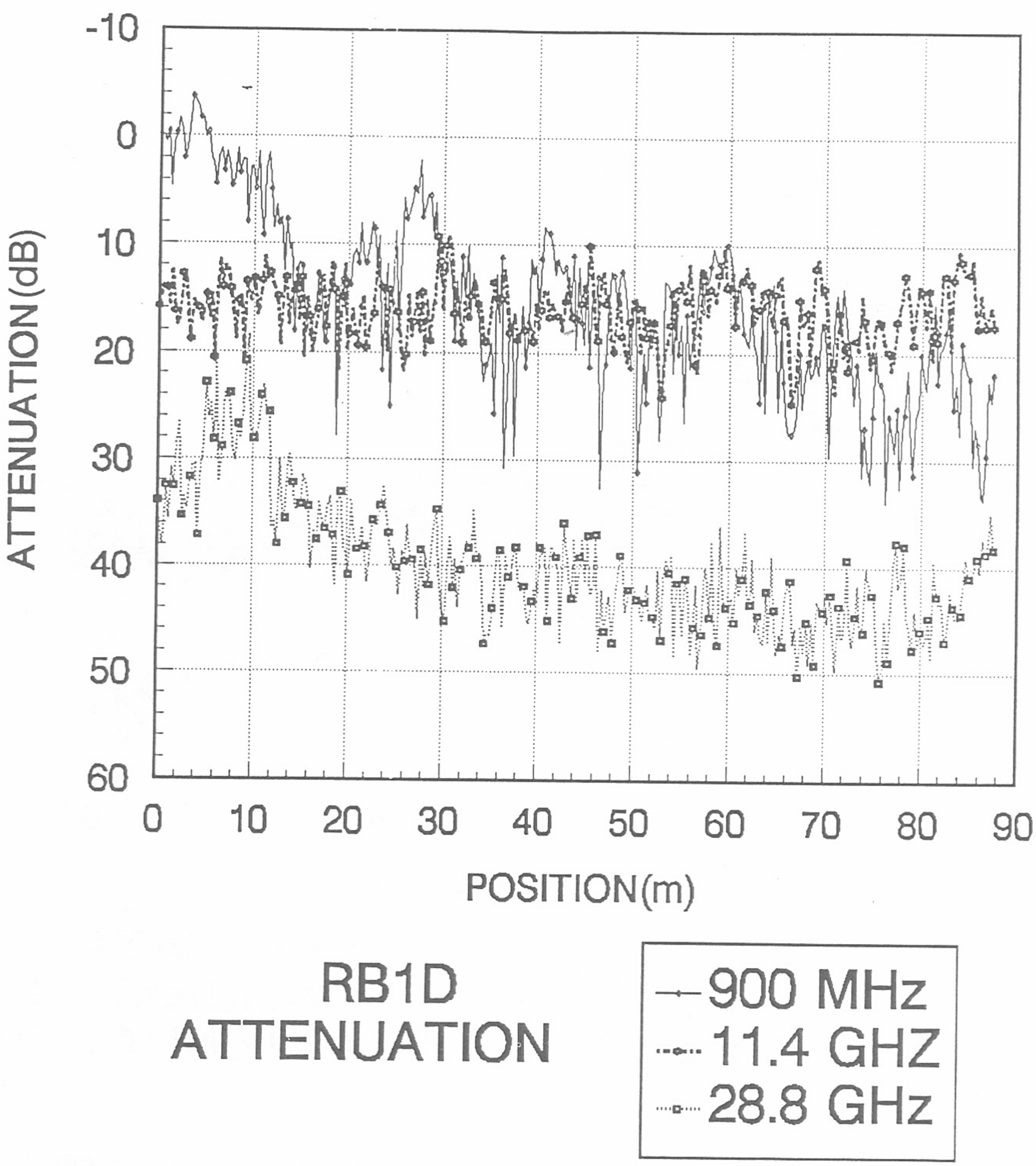

Figure 13. Penetration loss versus distance at three frequencies for a typical run in the Radio Building.

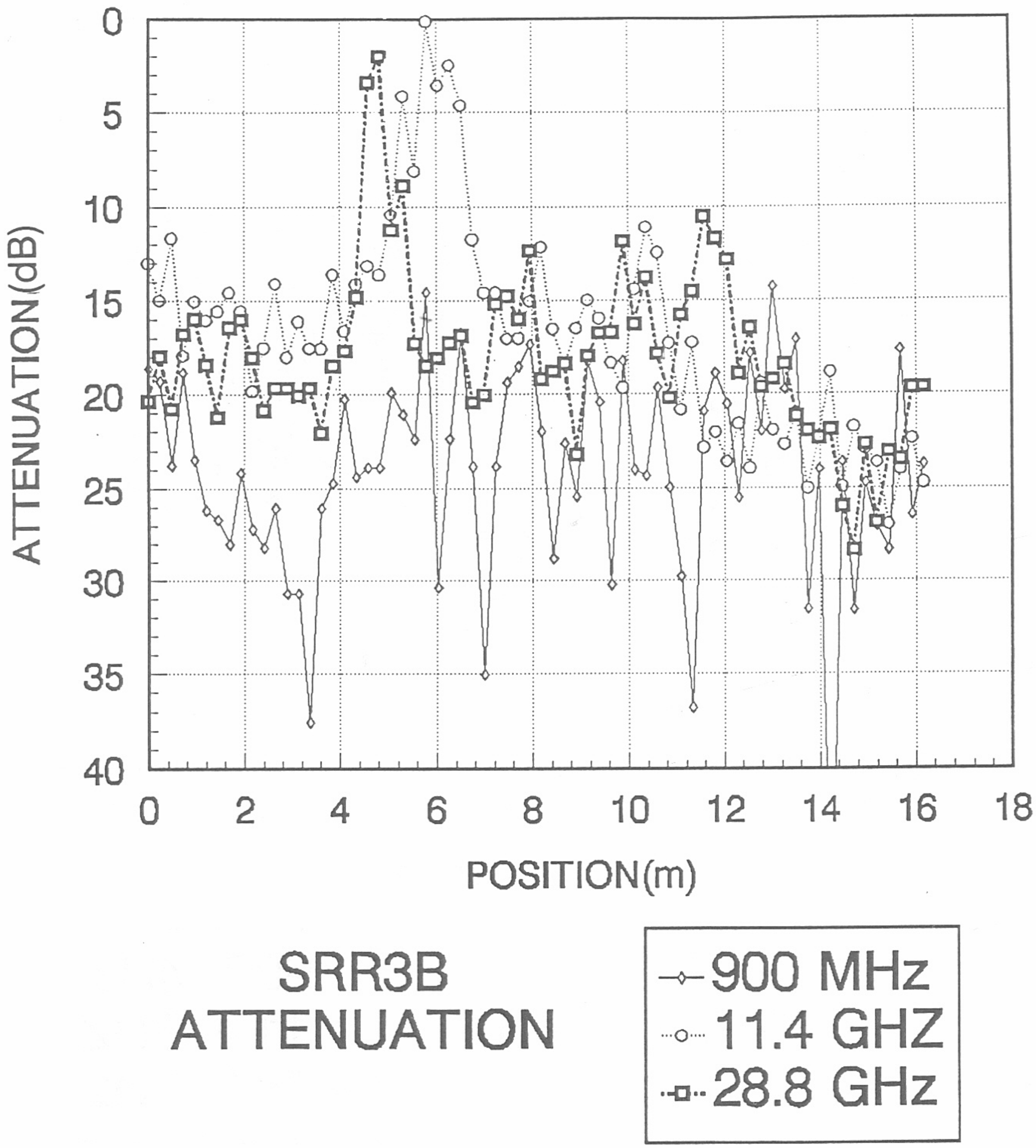

Figure 14. Penetration loss versus distance at three frequencies for a typical run in the storeroom building with metal siding.

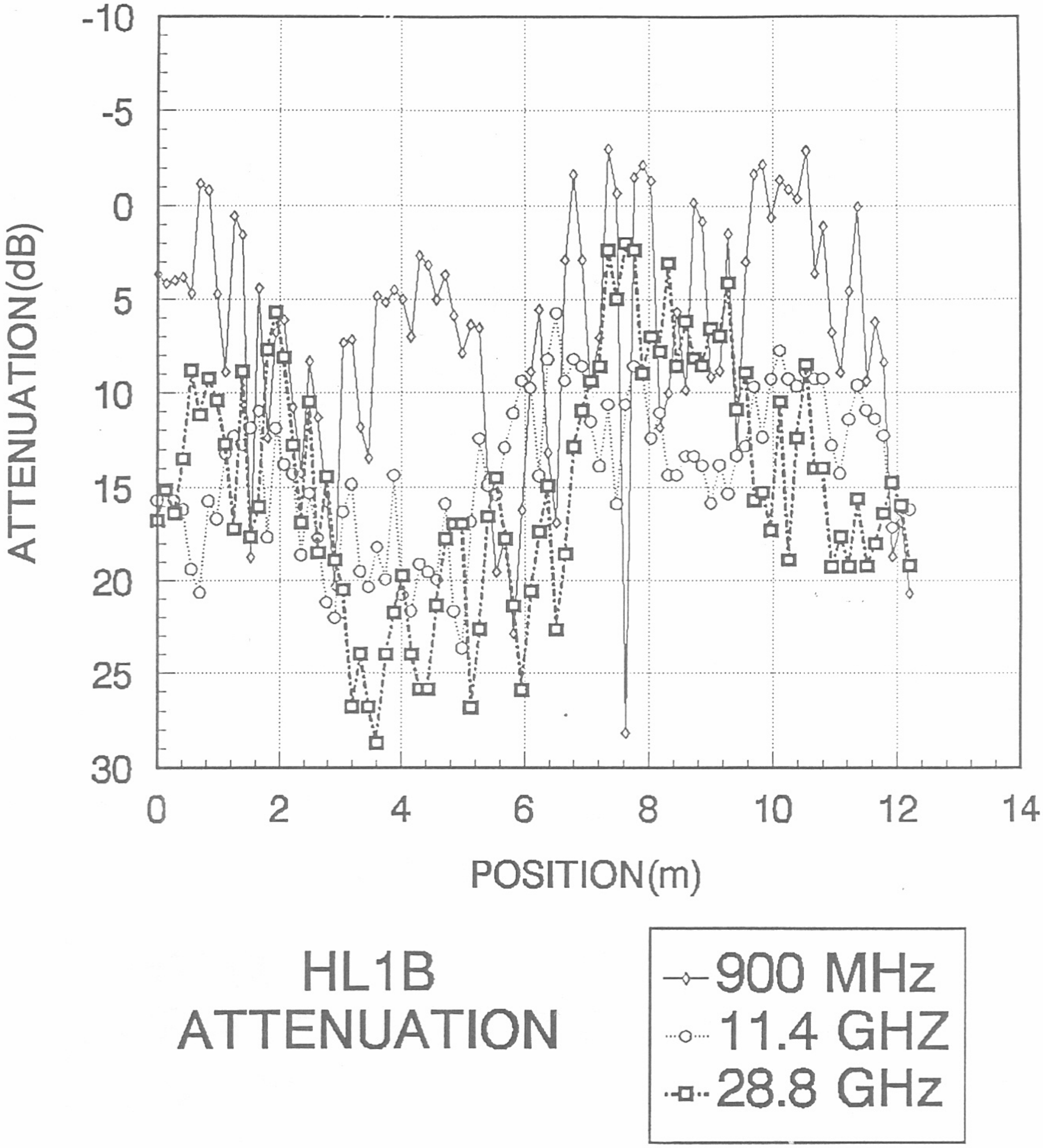

Figure 15. Penetration loss versus distance at three frequencies for a typical run in the private residence.

Table 1. Mean and Standard Deviation of attenuation (dB) for Radio Building Penetration Loss Path Data

	900 MHz		11. 4 GHz		28.8 GHz		
path	mean	stdev	mean	stdev	mean	stdev	comments
RB1D	15.3	8.2	16.0	2.8	39.6	6.2	main hall,van at end
RB1E	15.9	7.7	17.2	3.0	39.5	5.6	main hall,van at end
RB2B	29.2	5.3	33.9	4.0	52.5	1.5	Rm3430lab,van at end
RB2C	29.0	5.3	34.1	3.8	53.0	1.5	Rm3430lab,van at end
RB3B	28.0	4.6	35.6	2.7	53.5	1.3	Rm3430lab,van at end
RB3C	28.4	4.4	35.1	2.9	53.4	1.4	Rm3430lab,van at end
RB4C	29.4	5.5	31.1	3.4	53.8	3.5	Rm3454lab,van at end
RB4D	29.7	5.9	32.2	3.6	52.6	3.9	Rm3454lab,van at end
RB5A	27.9	5.4	37.6	1.9	54.6	2.2	Rm3454lab,van at end
RB5B	28.3	3.5	37.6	2.3	53.3	2.7	Rm3454lab,van at end
RB6A	20.0	3.9	32.1	1.6	42.7	2.5	Rm3453ofc,van at end
RB6B	19.6	5.0	30.7	2.3	41.9	4.1	Rm3453ofc,van at end
RB7A	20.9	5.7	31.3	1.2	42.1	3.5	Rm3453ofc,van at end
RB7B	21.2	5.0	31.6	1.8	41.5	2.4	Rm3453ofc,van at end
RB8A	9.4	6.1	5.9	2.3	4.1	0.8	Rm3467ofc,van on sdw
RB8B	8.7	6.6	5.7	2.5	3.9	0.8	Rm3467ofc,van on sdw
RB9A	11.1	6.2	3.8	2.3	3.3	1.2	Rm3467ofc,van on sdw
RB9B	10.0	5.9	3.1	1.3	3.2	1.1	Rm3467ofc,van on sdw
RB10A	5.5	4.5	3.8	2.0	6.0	2.3	Rm3453ofc,van on sdw
RB10B	8.1	7.3	2.9	1.5	4.9	1.5	Rm3453ofc,van on sdw
RB11A	11.2	5.6	2.9	1.9	4.3	1.1	Rm3453ofc,van on sdw
RB11B	9.3	6.2	2.3	1.8	4.2	1.0	Rm3453ofc,van on sdw
RB12A	9.9	5.8	4.6	2.4	6.6	2.6	Rm3447ofc,van on sdw
RB12B	9.6	6.5	4.7	3.6	6.5	2.8	Rm3447ofc,van on sdw
RB13A	11.3	5.3	4.3	2.1	5.0	1.4	Rm3447ofc,van on sdw
RB13B	7.8	6.1	3.5	2.0	4.7	1.3	Rm3447ofc,van on sdw
RB14A	7.3	5.0	3.0	1.9	6.4	2.0	Rm3443ofc,van on sdw
RB14B	8.4	4.5	3.1	2.0	6.2	1.3	Rm3443ofc,van on sdw
RB15A	11.3	5.6	5.2	2.9	8.8	3.8	Rm3443ofc,van on sdw
RB15B	11.0	6.4	5.2	3.3	7.4	3.5	Rm3443ofc,van on sdw
RB16A	17.7	4.9	18.9	3.6	26.8	4.0	Rm3454lab,van on sdw
RB16B	17.4	5.2	17.4	2.8	26.1	3.2	Rm3454lab,van on sdw
RB17A	20.4	6.5	16.2	2.5	21.9	3.1	Rm3454lab,van on sdw
RB17B	19.2	4.8	16.3	2.5	21.3	3.4	Rm3454lab,van on sdw
RB18A	21.3	7.5	31.3	3.0	43.3	4.1	Rm3430lab,van on sdw
RB18B	21.1	6.6	30.7	2.2	43.1	3.2	Rm3430lab,van on sdw
RB19A	16.3	5.0	29.8	1.9	41.7	2.9	Rm3430lab,van on sdw
RB19B	15.4	4.9	30.5	2.4	41.8	2.1	Rm3430lab,van on sdw

Table 2. Mean and Standard Deviation of attenuation for Private Residence Penetration Loss Path Data

	900 MHz		11.4 GHz		28.8 GHz		
path	mean	stdev	mean	stdev	mean	stdev	comments
HL1B	6.9	6.6	14.1	3.9	14.8	6.4	rear path, two walls
HL1C	6.3	6.5	13.3	4.0	14.1	6.6	rear path, two walls
HL2A	2.7	4.6	9.7	2.9	8.6	4.8	front path, one wall
HL2B	3.6	6.1	9.8	3.9	8.6	4.4	front path, one wall

Table 3. Mean and Standard Deviation of attenuation for Storeroom Penetration Loss Path Data

	900 MHz		11.4 GHz		28.8 GHz		
path	mean	stdev	mean	stdev	mean	stdev	comments
SRR1A	17.6	5.6	17.1	3.6	16.1	6.4	side aisle path
SRR1B	17.3	5.1	17.1	3.1	17.6	6.4	side aisle path
SRR2A	21.3	5.4	20.5	3.6	17.5	4.2	side aisle path
SRR2B	21.6	6.0	20.8	3.5	17.6	4.8	side aisle path
SRR3A	23.7	5.6	16.5	5.7	16.9	4.6	side aisle path
SRR3B	24.3	5.9	16.6	5.6	17.8	4.5	side aisle path
SRR4A	25.1	5.3	17.0	5.4	18.4	4.2	side aisle path
SRR4B	24.8	5.0	16.4	5.5	17.7	4.8	side aisle path
SRR5A	27.7	5.7	17.7	5.2	19.5	4.4	side aisle path
SRR5B	26.6	4.4	17.1	5.3	19.5	4.4	side aisle path
SRR6A	26.1	6.6	17.4	6.7	20.1	2.9	side aisle path
SRR6B	27.4	5.8	17.5	5.9	20.1	3.1	side aisle path
SRR7A	24.9	5.6	17.2	5.5	18.7	3.6	side aisle path
SRR7B	25.8	6.5	16.5	6.2	18.6	3.3	side aisle path
SRR8A	21.7	6.1	4.3	2.7	13.2	2.7	main aisle path
SRR8B	22.5	6.7	4.3	2.7	13.0	4.4	main aisle path

Table 4. Mean and Standard Deviation of attenuation for Building Penetration Loss for a Variety of Combinations of Data Paths

	900 MHz		11.4 GHz		28.8 GHz		File
	mean	stdev	mean	stdev	mean	stdev	
All Data In Radio Building Combined	17.7	9.3	19.8	11.5	34.1	17.4	ALLRB
All Data In Radio Building with Only One Wall Between XMTR And RCVR	9.4	6.1	4.1	2.6	5.6	2.7	RBOFF2
All Data In Radio Building with 2 Or 3 Walls Between XMTR And RCVR	18.9	6.4	26.0	7.0	36.2	9.5	RBLAB2
All Data In Radio Building With More Than 3 Walls Between XMTR And RCVR	28.8	5.1	34.4	3.8	53.3	2.4	RBLAB1
All Data In Private Residence Combined	5.4	6.4	12.3	4.3	12.4	6.6	ALLHL
All Data In Private Residence with One Wall Between XMTR And RCVR	3.2	5.4	9.7	3.5	8.6	4.6	HLFRNT
All Data In Private Residence With Two Walls Between XMTR And RCVR	6.6	6.6	13.7	4.0	14.5	6.6	HLREAR
All Data In Stockroom Combined	24.3	6.3	15.0	7.1	17.5	4.8	ALLSRR

each of these tables are also used to identify the paths in Figures 7, 8, and 9. Two runs are shown for each path. The letter suffix on the end of the path name separately identifies each of these path runs.

Cumulative distribution functions of certain files or combinations of files representing certain communications scenarios were performed to look at the statistics of the particular situation.

An example of one practical situation would be an evaluation of communications capability from anywhere in an office building (Radio Building) for a fixed external base station (represented by the van). This would require combining all of the separate files taken in that building. Figure 16 is a cumulative distribution function for all the data in the Radio Building. Analyzing all data files would allow determination of the link margin necessary for designing Personal Communication Systems using these higher frequencies. Figure 16 shows the cumulative distribution function for all of the Radio Building data at the three frequencies. This figure indicates that less than 0.1 % of the data points will have penetration attenuation of more than 47 dB at 900 MHz, 41 dB at 11.4 GHz, and 58 dB at 28.8 GHz.

Figure 16 is a composite of a large amount of data representing many diverse conditions. Some measurement points on certain data paths had one wall present between the transmitter and the receiver, but other data contains paths with more than three walls between the transmitter and the receiver. Figure 17 contains data paths where only one wall separates the transmitter and receiver in the Radio Building. This wall had a lot of window area. The mean attenuation is much smaller (less than 10 dB). The attenuation was more than 28 dB at 900 MHz, 13 dB at 11.4 GHz, and 16 dB at 28.8 GHz less than 0.1 % of the time. Figure 18 contains data paths with two or three walls between the transmitter and the receiver. The mean attenuation can be as great as 39 dB. Figure 19 contains path data where more than three walls are involved and the mean attenuation can be as high as 53 dB.

Table 4 contains the mean attenuation and its standard deviation for all of these cases. All of these separate cases for the Radio Building indicate an increasing penetration attenuation at all frequencies as the number of wall penetrations increases in the building structure. This behavior was noted in the data taken for the private residence (wood-frame structure with brick veneer). Figure 20 is the cumulative distribution function of the combined data for all of the paths in the private residence. Figure 21 is the cumulative distribution function for the condition of one wall separation between the transmitter and receiver (front hallway traverse). Figure 22 is for the case of two wall separations (rear hallway traverse). Figure 23 is for the case of one wall separation in the storeroom. Data was not collected for the case of more than one wall separation for the storeroom.

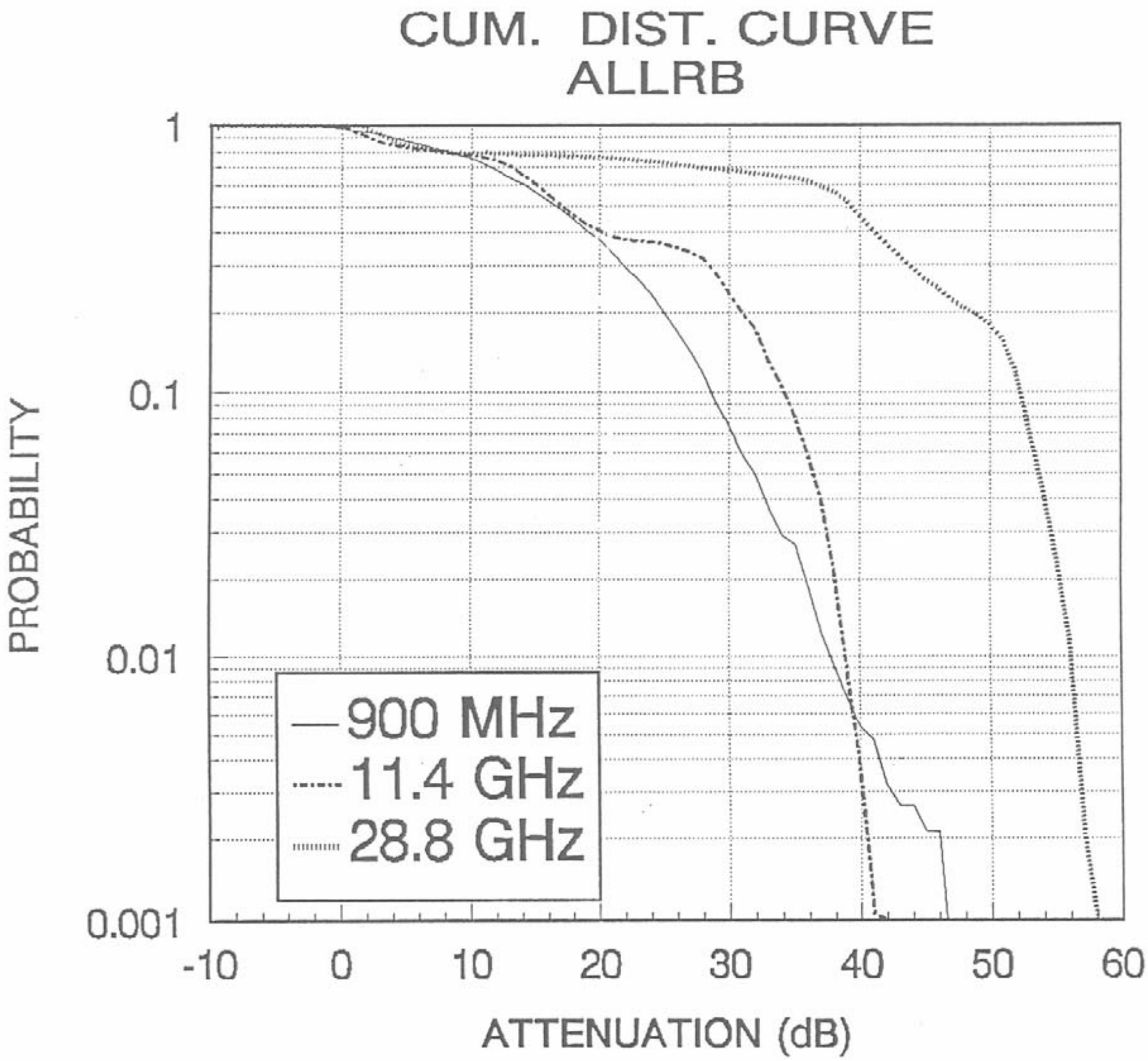

Figure 16. Cumulative distribution for all data in the Radio Building.

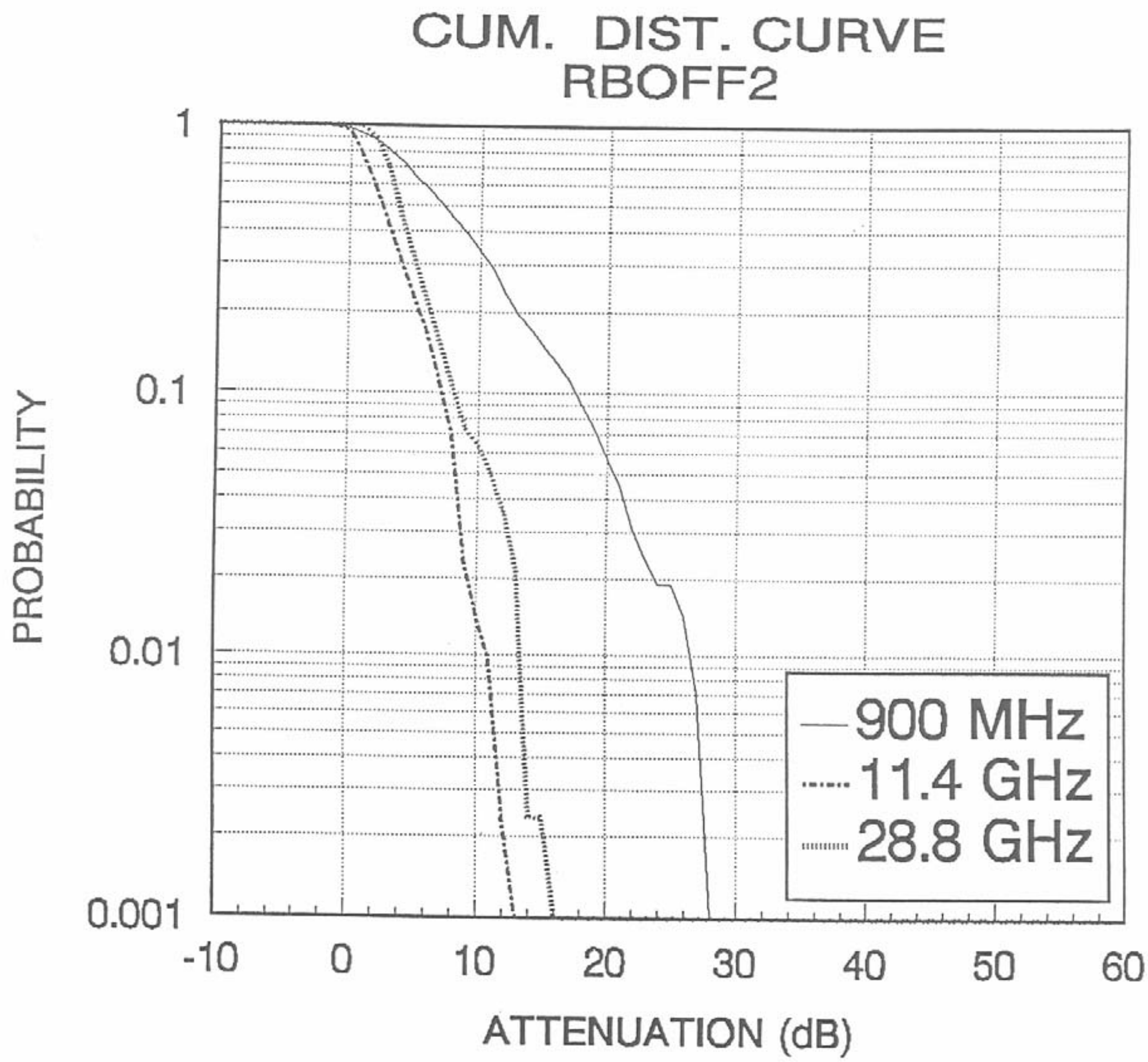

Figure 17. Cumulative distribution for all data in the Radio Building with just one wall between the transmitter and receiver.

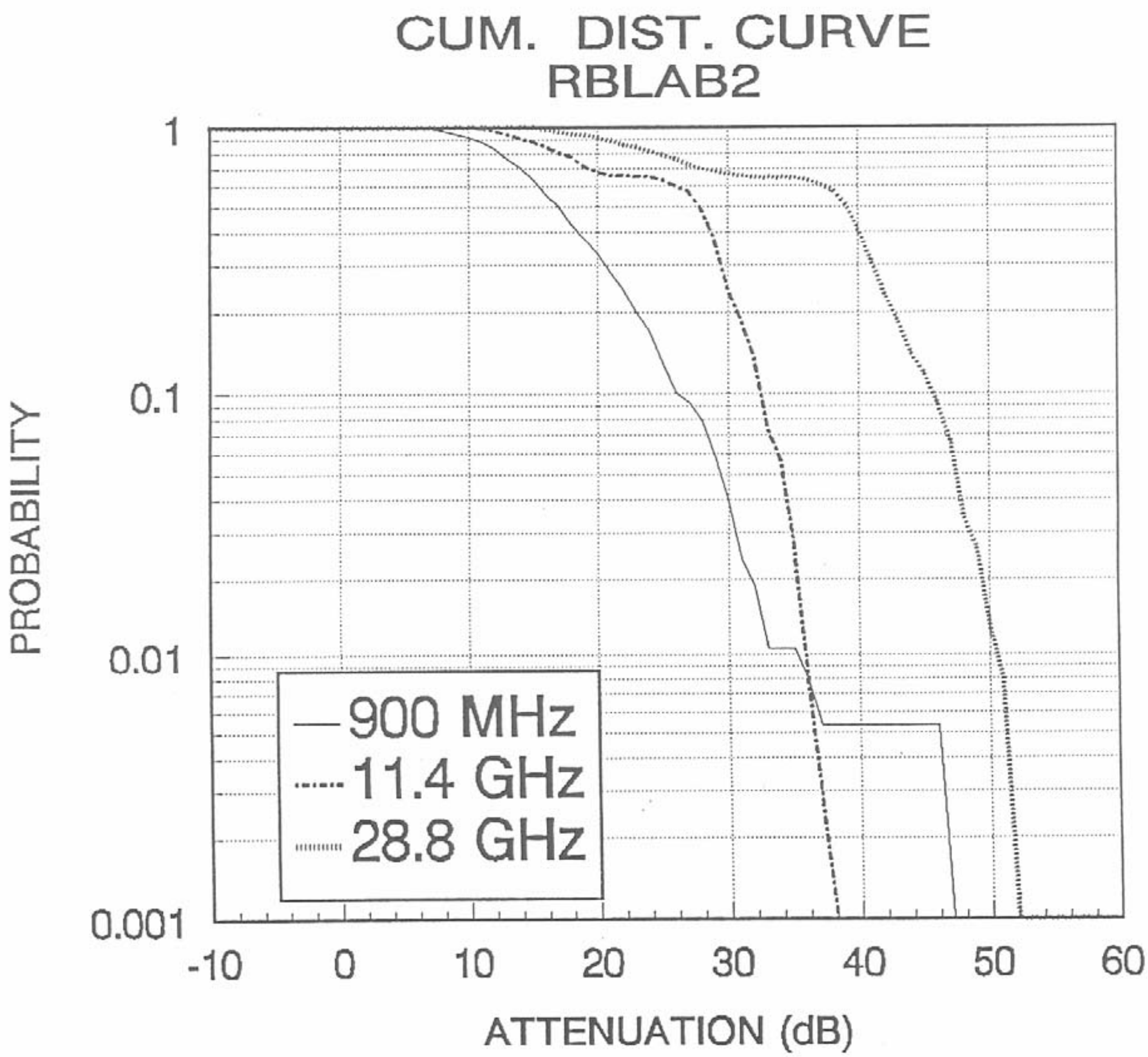

Figure 18. Cumulative distribution for all data in Radio Building with two or three walls between the transmitter and receiver.

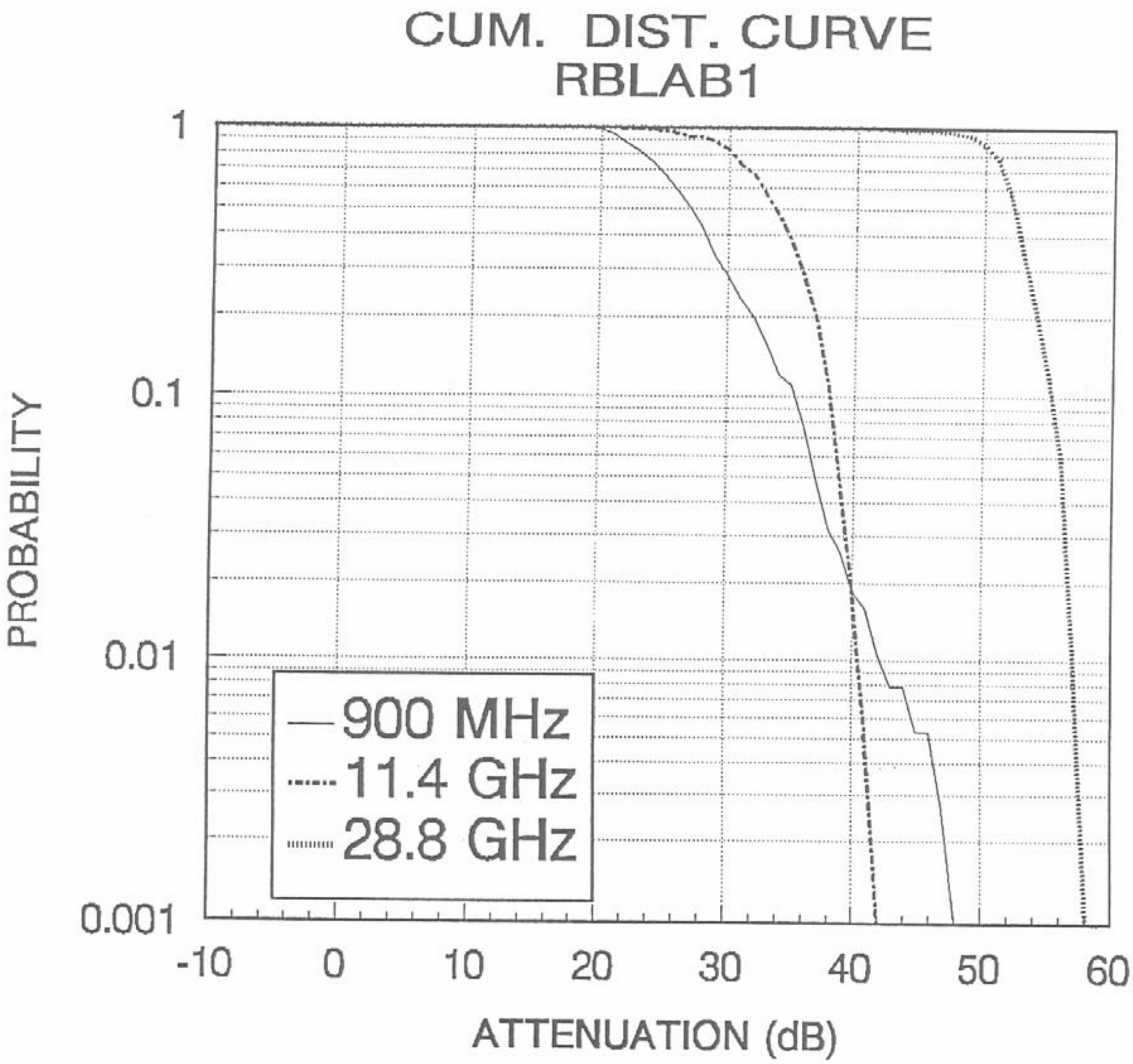

Figure 19. Cumulative distribution for all data in Radio Building with three or more walls between the transmitter and receiver.

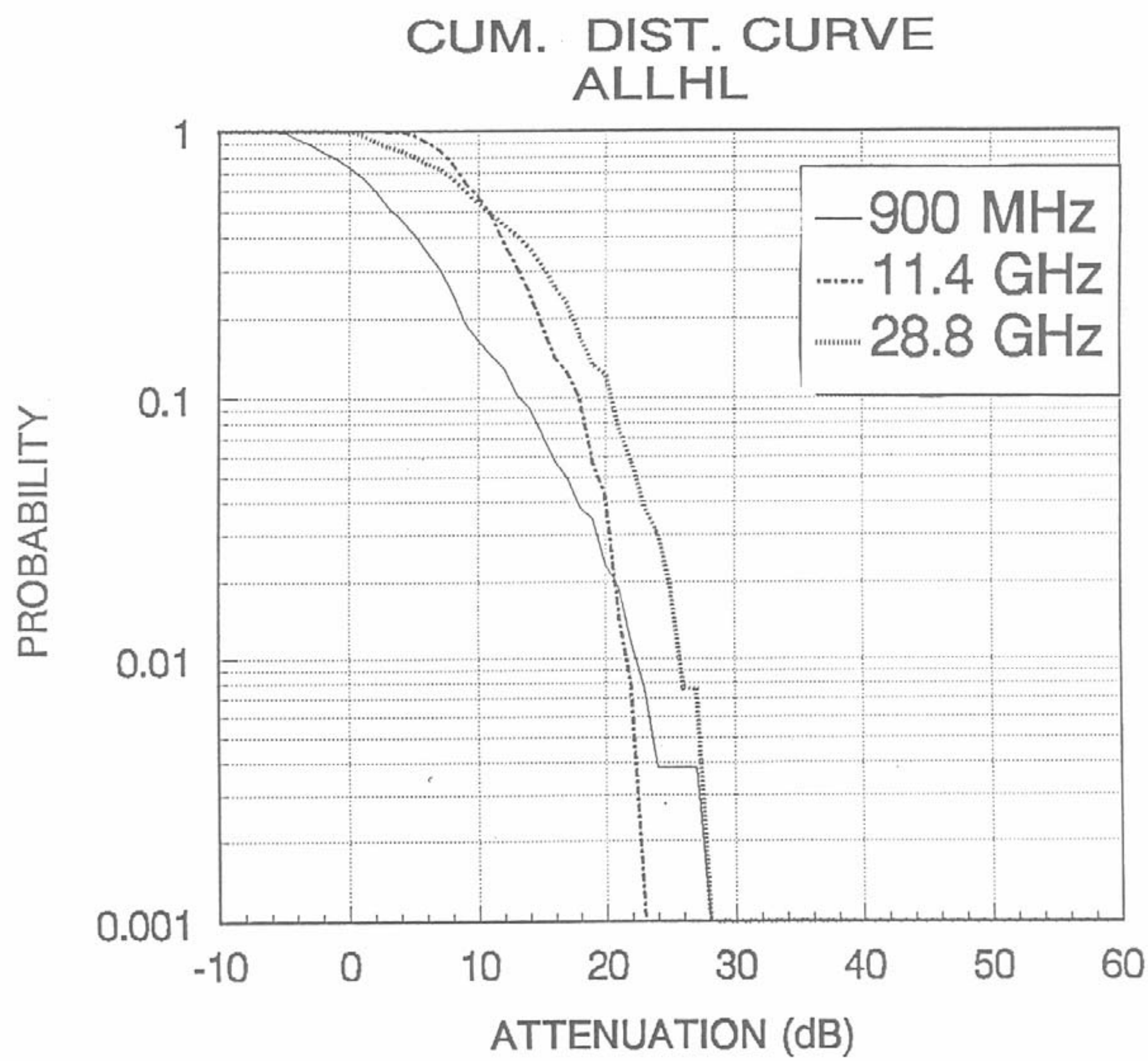

Figure 20. Cumulative distribution for all data in the private residence.

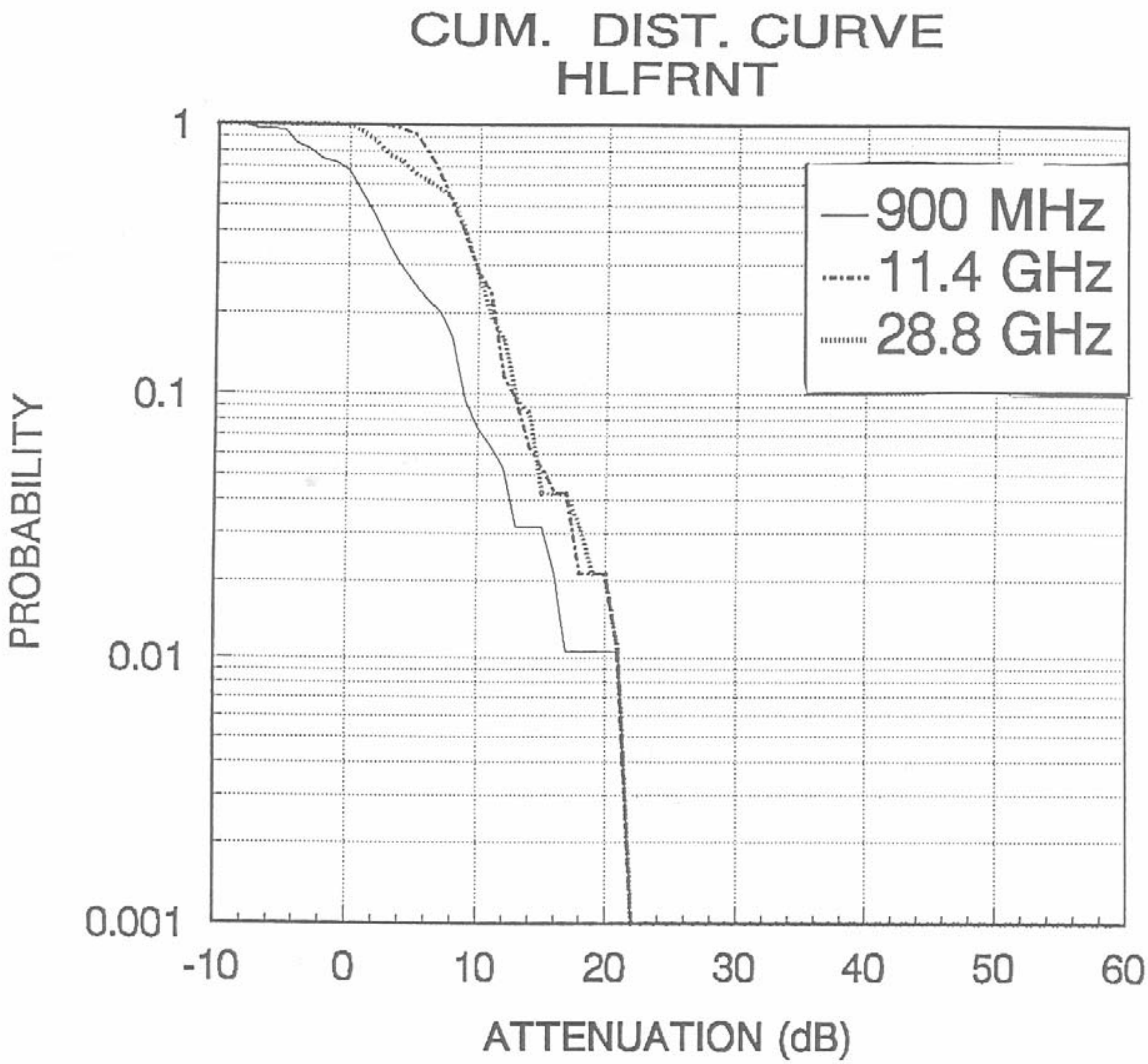

Figure 21. Cumulative distribution for all data in the private residence with one wall between the transmitter and receiver.

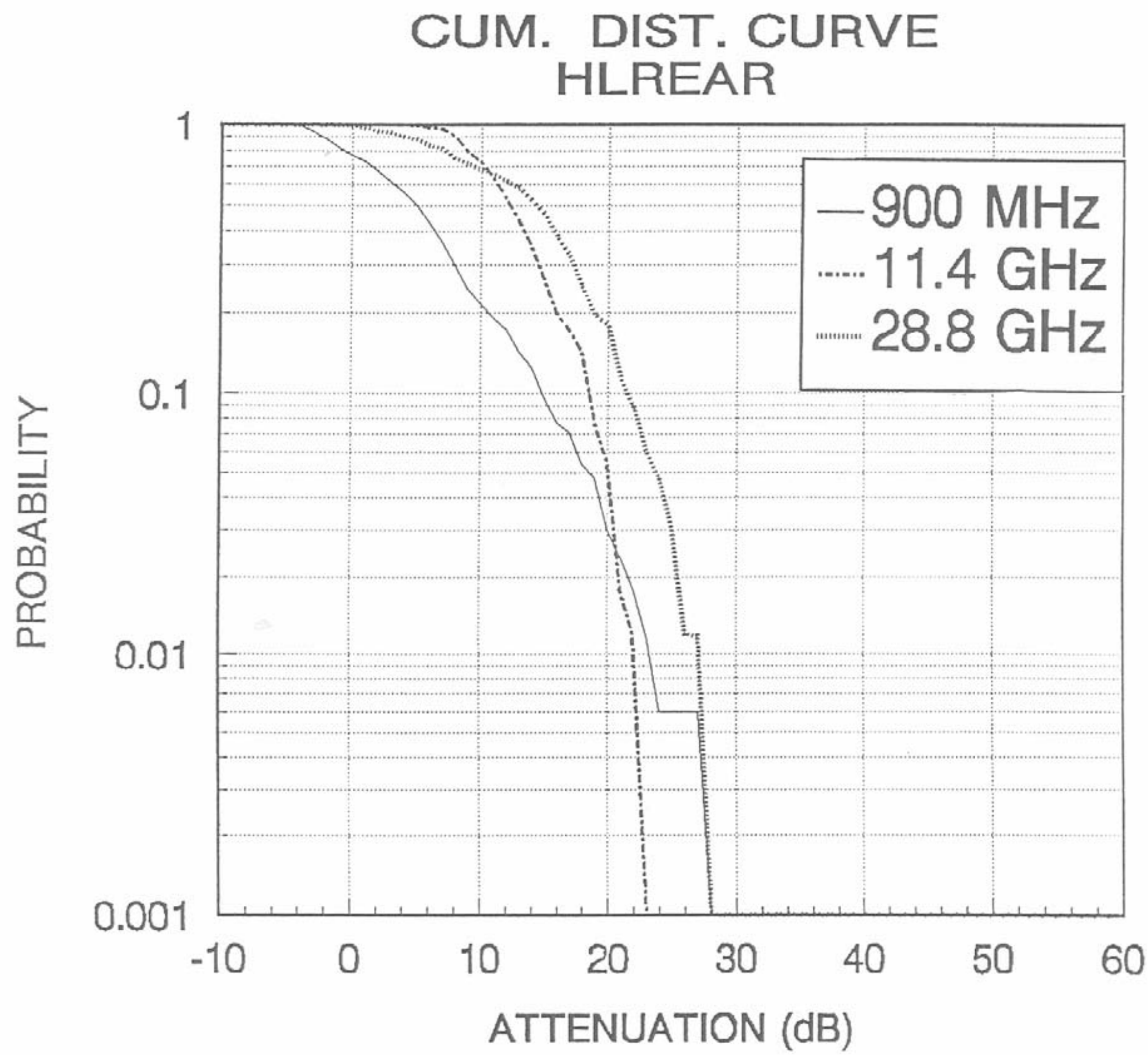

Figure 22. Cumulative distribution for all data in the private residence with two walls between the transmitter and receiver.

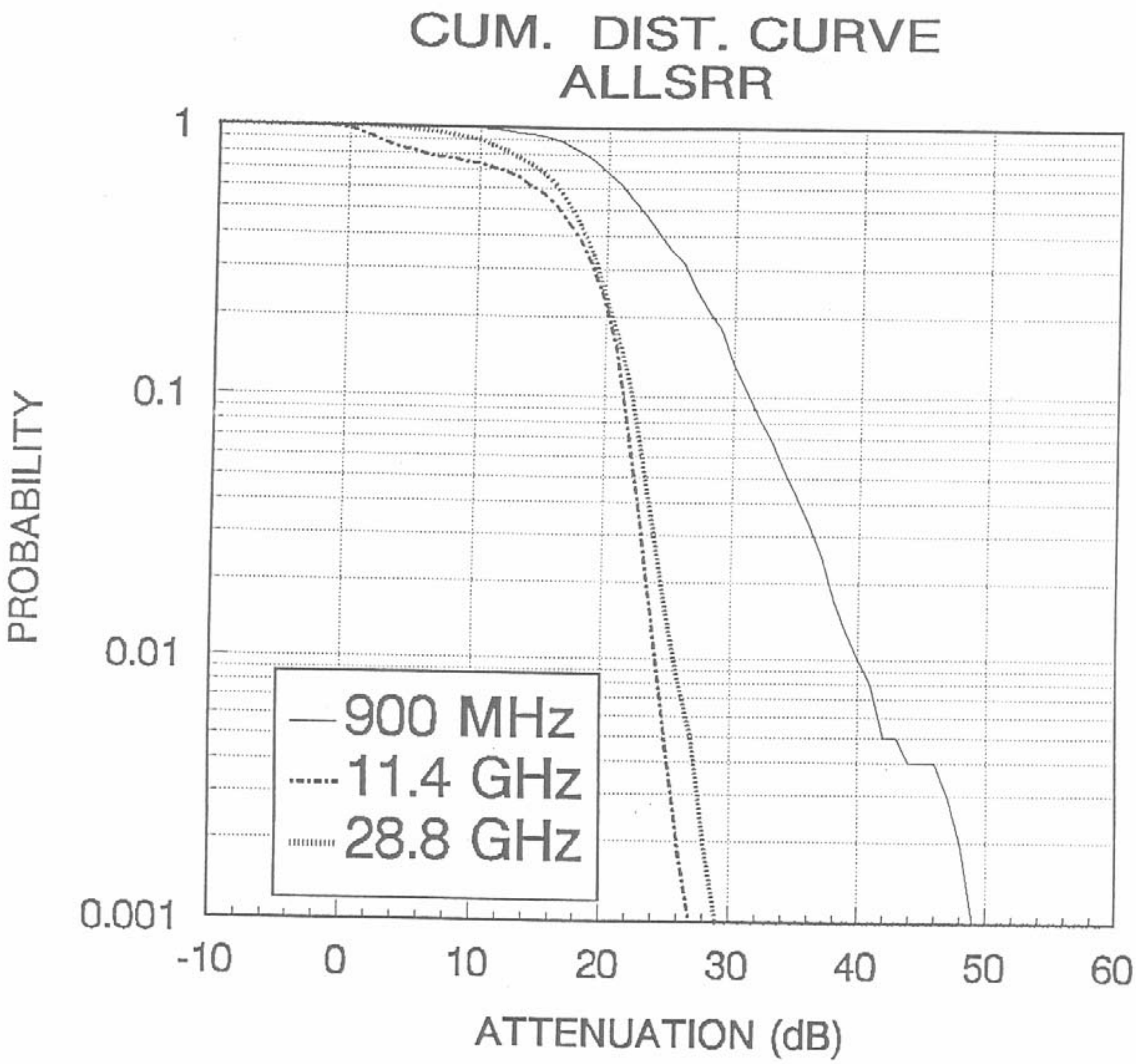

Figure 23. Cumulative distribution for all data in the storeroom building with metal siding.

The maximum attenuation that will be present less than a certain percentage of time can be read off these figures. This number can be used for the link margin at different link reliabilities. Table 4 has the mean attenuation and its standard deviation for all three data combinations. The means at all frequencies are greater for the two-wall case.

Figure 23 shows the cumulative distribution function for all of the data collected in the storeroom (metal structure with metal siding). The mean attenuation and its standard deviation are listed in Table 4. The attenuation is highest (greater than 49 dB less than 0.1 % of the time) at 900 MHz, because of the shielding effect of the metal siding on the building and the small windows (with respect to a wavelength at 900 MHz). The attenuation at 11.4 and 28.8 GHz was greater than 27 and 29 dB respectively less than 0.1 % of the time.

6.0 CONCLUSIONS

The penetration attenuation for the Radio Building and the private residence tend to increase with frequency. The penetration attenuation for the storeroom decreases with increasing frequency.

The separate cases for the Radio Building and private residence also indicate a progressively increasing amount of penetration attenuation at all frequencies as the number of wall penetrations increase in the building structure.

The electromagnetic energy at 11.4 and 28.8 GHz can couple into the storeroom building more effectively than that energy at 900 MHz. The shielding effectiveness (ratio in dB of the power outside the structure to the power inside the structure) of the structure is less at the two higher frequencies and allows more energy to couple through the walls. The shielding effectiveness of a metal structure is dependent on the size of the openings in the outer shell of the structure. These may be windows, doors, heating and/or air conditioning penetrations, holes, etc. When the size of the opening in the structure is greater than or comparable to a wavelength, then the opening in the structure provides a strong coupling path for electromagnetic energy to flow into or out of the structure. This reduces the penetration attenuation of the structure.

The penetration attenuation values derived from the measurements conducted in this study can be used determine the feasibility of personal communications. The cumulative distribution functions of the penetration attenuation can provide information on what link margins are necessary for different communication probabilities or reliabilities. The penetration attenuation provides a quantitative margin for link calculations to use in analyzing and designing personal communication systems.